The Journal of Chemical Physics

High pressure behavior of ethylene and water: From clathrate hydrate to polymerization in solid ice mixtures

Cite as: J. Chem. Phys. **158**, 064505 (2023); https://doi.org/10.1063/5.0137863
Submitted: 06 December 2022 • Accepted: 22 January 2023 • Accepted Manuscript Online: 23 January 2023 • Published Online: 09 February 2023

S. Berni, D. Scelta, S. Fanetti, et al.

AIP Publishing

The Journal of Chemical Physics ARTICLE scitation.org/journal/jcp

High pressure behavior of ethylene and water: From clathrate hydrate to polymerization in solid ice mixtures

Cite as: J. Chem. Phys. 158, 064505 (2023); doi: 10.1063/5.0137863
Submitted: 6 December 2022 • Accepted: 22 January 2023 •
Published Online: 9 February 2023

S. Berni,[1,2] D. Scelta,[1,3,a)] S. Fanetti,[1,3] and R. Bini[1,2]

AFFILIATIONS

[1] LENS, European Laboratory for Non-linear Spectroscopy, Via N. Carrara 1, I-50019 Sesto Fiorentino, Firenze, Italy
[2] Dipartimento di Chimica "Ugo Schiff" dell'Università degli Studi di Firenze, Via della Lastruccia 3, I-50019 Sesto Fiorentino, Firenze, Italy
[3] ICCOM-CNR, Institute of Chemistry of OrganoMetallic Compounds, National Research Council of Italy, Via Madonna del Piano 10, I-50019 Sesto Fiorentino, Firenze, Italy

[a)] **Author to whom correspondence should be addressed:** scelta@lens.unifi.it

ABSTRACT

Among the ice mixtures that can be found in our universe, those involving ethylene are poorly studied even though ethylene reportedly exists in the presence of water in several astrochemical domains. Here, we report on the chemistry of ethylene and water mixtures in both pressure (0–15 GPa) and temperature (300–370 K) ranges relevant to celestial bodies conditions. The behavior of the binary mixture has been tracked, starting from the ethylene clathrate hydrate and following its evolution through two different crystalline phases up to 2.10 GPa, where it decomposes into a solid mixture of water ice and crystalline ethylene. The pressure and temperature evolution of this mixture has been studied up to the complete transformation of ethylene into polyethylene and compared with that of the pure hydrocarbon, reporting here for the first time its spectroscopic features upon compression. The spectroscopic analysis of the recovered polymers from the ice mixtures provided hints about the reactivity of the monomer under the environmental stress exerted by the water network. The results of this study are expected to be significant in a variety of fields ranging from astrochemistry to material science and also to fundamental chemistry, particularly regarding the study and modelization of the behavior of complex mixtures.

I. INTRODUCTION

Water is one of the most widely distributed molecules in our universe: it can be found in the gas phase in the interstellar and circumstellar clouds,[1] less commonly as a solid, mainly on icy bodies such as giant planets satellites[2,3] and Kuiper belt objects,[4] and occasionally as a liquid, a form of paramount importance for the chemistry of life. Carbon-bearing molecules are also widespread chemicals. Indeed, liquid hydrocarbons exist on many icy bodies in our solar system, such as on the surface of Titan or in the subterranean oceans on Enceladus. More generally, liquid and solid hydrocarbons can be found where the atmosphere is cold enough to let them condense.[5,6] In addition, a large variety of differently sized carbon compounds have been detected on cometary comae[7] or reproduced in experimental simulations of cometary analogs,[8] and very complex carbon-based compounds such as polycyclic aromatic hydrocarbons (PAHs) or long-chain polymers are typical carbonaceous constituents of meteorites.[5] The simultaneous presence of water and hydrocarbons has, therefore, primary importance in diverse astronomical contexts, ranging from the above-mentioned cometary comae to the atmospheres, crusts, and first layers of many satellites and planetoids. The coexistence of water and small hydrocarbons manifests itself as solid ice mixtures, polyphasic systems made up of variously segregated solid constituents, or, quite often, through the formation of supramolecular compounds such as clathrate hydrates.

Besides that of methane, probably the most common hydrocarbon to be found alone and in combination with water in icy mixtures across the solar system, the case of ethylene presents a peculiar interest for fundamental chemistry, being C_2H_4 the

simplest double-bonded hydrocarbon. Ethylene is usually studied in material chemistry for its polymerization product, polyethylene, a compound of major interest with a huge variety of technological applications, from thermoplastics to medical prostheses implantation.[9] The presence of ethylene in astronomical environments has been reported for several giant planets and icy bodies in the form of evaporites,[10] dissolved in CH_4/C_2H_6 lakes[11] or, mainly, as a gas in their upper atmospheres.[12–14] In this framework, ethylene is synthesized during the photolysis of other hydrocarbons, typically methane, and it is involved in the complex reaction pathways leading to the formation and decomposition of ethane.[12,14,15] Just like methane or ethane, C_2H_4 is expected to play a role in the peculiar chemistry happening on Titan, but it is also present on other icy bodies and planetoids of the outer solar system and their atmospheres, such as in the case of Pluto[16] and Makemake.[15] Moreover, ethylene was also observed as a product formed following the impact of the Shoemaker–Levy comet into Jupiter's atmosphere.[17]

The high pressure behavior of ethylene has been extensively studied in the past few years. The Raman spectra of liquid and solid ethylene have been studied at low temperatures and atmospheric pressure,[18,19] but no reports are available at high pressure. On the contrary, the infrared spectrum of ethylene has been studied under pressure, and it has been successfully employed to follow and study ethylene polymerization. The reaction is reported to occur at 3.60 GPa in the solid phase upon simple compression[20] and has been extensively studied also in the liquid phase under various wavelength irradiations[21,22] and as a function of temperature.[23]

On the other hand, the ethylene–water ice mixtures are far less studied in the laboratory. Only a few works have been published over the years, mainly focusing on ethylene clathrate hydrate and particularly on the low pressure–low temperature phases. The clathrate hydrate spectral features have been investigated via Raman[24] and infrared spectroscopies,[25] paying attention to the stability boundaries and small cage occupancy in the lower pressure phase[26] and, in more recent times, to the refinement of its crystalline structure.[27] In any case, these studies were devoted to understanding the influence of ethylene on methane–water ice mixtures and on the stability of methane clathrate hydrate[24] or to providing reference spectra to be compared with remote observations.[25]

Here, we report a comprehensive high pressure–high temperature study of the ethylene–water mixture that encompasses both its ethylene clathrate hydrate form and its behavior at higher pressures, where the clathrate hydrate decomposes into water ice and crystalline ethylene. First, we characterized the whole Raman spectrum of ethylene clathrate hydrate in all its phases. Then, we focused on the Raman features of ethylene in solid mixtures with water ice, comparing them with those of pure ethylene samples, which have never been reported so far. In addition, we characterized the reaction threshold for the polymerization of ethylene in the presence of water, and finally, we analyzed the recovered polyethylenes obtained from these mixtures. Besides providing a deeper knowledge of the fundamental chemistry of ethylene alone and in combination with water, these studies are pivotal to obtaining a deeper understanding of the behavior of ice mixtures involving ethylene in the extreme pressure-temperature conditions that may occur in the interior of icy bodies in our solar system. Moreover, they are of great interest from the perspective of material chemistry in order to synthesize very low density polymers for possible technological applications.

II. EXPERIMENTAL

Crystalline ethylene clathrate hydrate was prepared by means of a specifically designed high pressure stainless steel vessel, as described elsewhere.[28] The vessel was filled with finely grounded ice, sealed using silver plated gaskets, and then cooled down to 240 K in an ethylene glycol bath using a chiller. The system was pumped for at least 12 h before 20 bars of ethylene (Sapio, 99.5%) were loaded, while maintaining the vessel at 240 K. Once the temperature stabilized, a temperature program was applied: starting from 262 K, the temperature was increased in 3 h to 267 K and then in 3 more hours to 272.65 K. In the final step, the temperature was slowly increased up to 273.65 K in 15 h. During the temperature program, the gas pressure increased up to 70 bars (at 262 K) and then decreased to 40 bars after the cycle completion. The vessel was unsealed under liquid nitrogen to collect the sample. The product appeared as white fine flakes, flammable, and highly unstable at room conditions.

Membrane Diamond Anvil Cells (mDACs) were employed to pressurize and study the samples. The mDACs were equipped with IIa type diamonds having culets with a range of diameters from 400 to 1000 μm, depending on the experimental purposes. The samples were enclosed by stainless steel gaskets with an initial diameter and thickness of about 150 and 50 μm, respectively (for 400 μm culet mDACs), and of about 500 and 140 μm (for 1000 μm culet mDACs). Ruby chips were used as pressure gauges.[29,30] The clathrate samples were transferred into the diamond anvil cells while maintaining them under cryogenic conditions. Once loaded into DACs, the samples were sealed by the application of helium pressure to the membrane and studied via Raman spectroscopy.

The pure ethylene samples were loaded using either the standard cryo-loading technique (28 bars, 243 K) or *spray-loading*, following the procedure described elsewhere.[31]

Raman spectra were measured in backscattering geometry by focusing a few mW of the 660 nm line of a solid state diode laser (Laser Quantum Torus) onto the sample through a long working distance 20× Mitutoyo micro-objective, providing a beam spot diameter of 2–3 μm. The high spatial resolution of the Raman equipment, together with the complete automation of the DAC stage (remotely controlled via software), allowed to perform grid acquisitions on the samples (Raman mappings): in this procedure, a certain number of Raman acquisitions can be performed at definite positions on a square mesh of desired dimensions. The unpolarized scattered light was dispersed by a single stage monochromator (Acton/SpectraPro 2500i), equipped with holographic super notch filters, and collected by a CCD detector (Princeton Instruments Spec-10:100BR). The typical resulting instrumental resolution was 0.6 cm^{-1} with the employed wavelength.[32] High temperature Raman spectra were collected using a specifically designed vacuum chamber for resistive heated DAC.[33] Raman data were analyzed using Fityk software.[34]

FTIR absorption measurements were performed using a Bruker-IFS 120 HR spectrometer suitably modified for high pressure and high temperature experiments,[35] using an MCT detector and a KBr beam splitter with an instrumental resolution of 1 cm^{-1}.

Angle dispersive x-ray powder diffraction (XRD) patterns were acquired at LENS on the recovered samples using a Xenocs-GeniX Mo Small Spot microsource (λ = 0.710 73 Å) equipped with multilayered focusing mirrors and collected on a PI-SCX 4300 CCD detector. The beam spot focal size was 100 μm with a typical acquisition time of 2 h. The 2D diffraction patterns were treated by software to remove the cosmic rays and then analyzed and integrated using DIOPTAS software.[36]

III. RESULTS AND DISCUSSION

The samples of ethylene clathrate hydrate were loaded into the DACs immediately after being synthesized, as described in Sec. II. We managed to load the samples at the lowest possible pressure; the samples were mapped and analyzed by Raman spectroscopy and then compressed to follow their pressure evolution.

A. Phase changes

Figure 1 reports optical photographs acquired on ethylene clathrate hydrate at various stages of compression. Figure 2 reports the Raman spectra of ethylene clathrate hydrate (full lines) and of pure ethylene (dotted lines) in the relevant spectral windows, collected at room temperature upon compression. To our knowledge, the spectra shown in Fig. 2 are the first reported in scientific literature covering the whole spectral range, besides the –C–H stretching region. Finally, Fig. 3 shows the pressure evolution of the peak frequencies for the Raman bands of encaged ethylene molecules in the diverse phases of ethylene clathrate hydrate (colored circles) compared with those of pure ethylene (open black squares). The photographs, the spectra, and the pressure evolutions of the frequencies show clear evidence of at least two different main transformations occurring in the pressurized samples, and it is noteworthy that these transformations can be interpreted quite differently from the existing literature.[24]

In good agreement with previous literature data, the first clathrate hydrate phase, called EH-I, was observed from the lowest pressure we accessed in these experiments, 0.20 GPa, up to 1.60 GPa. This phase is characterized by a typical doublet in the C=C stretching, –C–H stretching, and –CH_2 scissoring regions (see blue spectra in the left, central, and right panels of Fig. 2). As explained elsewhere,[26] the splitting of the bands is due to the occupancy of two different types of cages in the EH-I structure. EH-I features an sI-type structure[25,27] with small (5^{12}, S-cages) and medium ($5^{12}6^2$, M-cages) sized cages; the lower frequency peak in the spectra refers to the occupation of M-cages, while the higher frequency component refers to the occupation of S-cages.[25,26] Meanwhile, the dimensions of the ethylene molecule would seem to preclude its presence in the smaller 5^{12} cages of the sI-type structure, ethylene has been reported to occupy these cavities under pressure by virtue of framework deformations.[25,27] On the other hand, occupancy by ethylene of the larger $5^{12}6^2$ cages is favored. Thus, in reasonable agreement with recent findings about the cage occupation in the sI structure of ethylene clathrate hydrate[27] and with reports for the sI structure in analogous systems such as methane clathrate hydrate,[37] we observed that the intensity ratio for all the split doublets in EH-I is close to 3:1.

At 1.60 GPa, ethylene clathrate hydrate undergoes its first transformation; here, the Raman spectrum reflects the coexistence of the EH-I phase together with the incoming EH-II phase. The transition between the two phases is quite sluggish, and EH-I can be overcompressed up to 1.75 GPa, thus defining a coexistence domain that extends from 1.60 to 1.75 GPa. Once the sample has completed its transformation, a small pressure drop to 1.60 GPa is observed. The structural change is highlighted by the different textures characterizing the sample [see photos (a) referring to EH-I and (b) referring to EH-II, in Fig. 1]. From a spectroscopic point of view, the transition and the related coexistence region are characterized by the growth of a new peak in between the doublet of phase EH-I relative to the C=C stretching mode (yellow curve in the central panel of Fig. 2), while in the –CH_2 scissoring region and, more evidently, in the –C–H stretching region, we observe a superposition of the EH-I spectrum with the spectral features of the EH-II spectrum. This can be easily seen by comparing the yellow curves in the left and right panels of Fig. 2 with the blue and red ones related to EH-I and EH-II, respectively.

Once the transition is completed, the measured Raman spectrum, which is ascribed to the EH-II phase of ethylene clathrate hydrate, shows broad and asymmetric bands for the –CH_2 scissoring

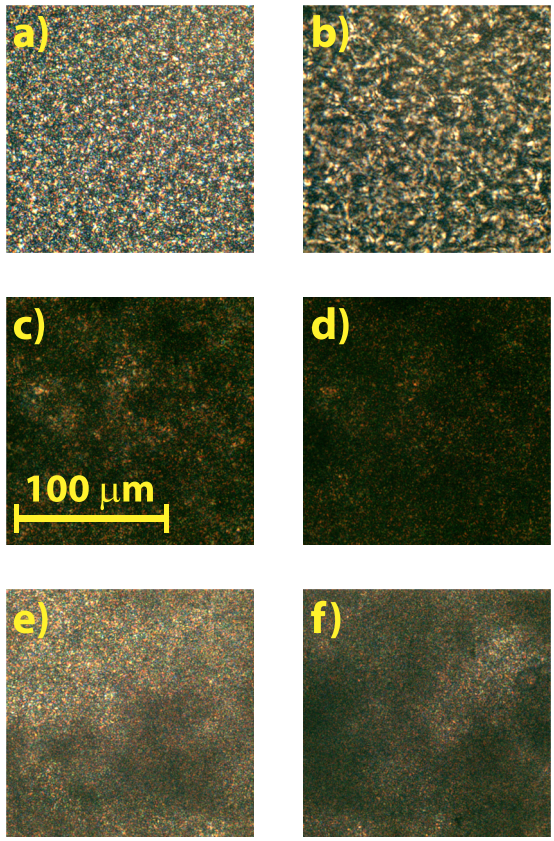

FIG. 1. Microscope photographs of the ethylene clathrate hydrate sample at various stages of compression: (a) 0.60 GPa, EH-I phase; (b) 1.60 GPa, EH-II phase; (c) getting darker upon compression at about 2 GPa; (d) at 2.10 GPa; (e) decomposed Ice-VII and plastic C_2H_4-II at 2.60 GPa; (f) decomposed Ice-VII and crystalline C_2H_4-I at 3.30 GPa. Photographs were acquired with transmitted like.

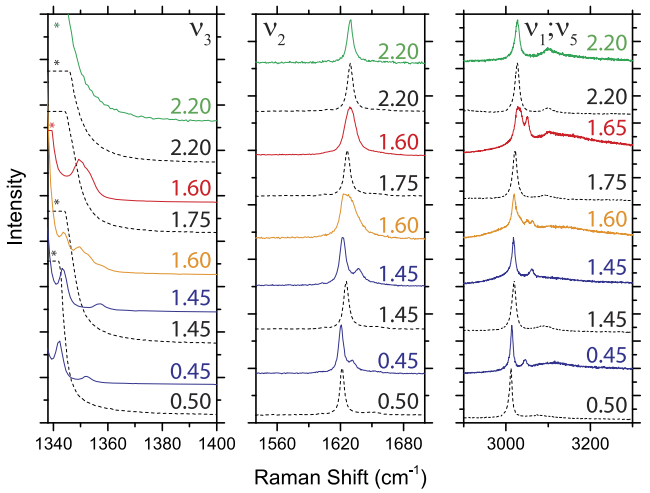

FIG. 2. Raman spectra of ethylene clathrate hydrate at various pressures. Colors mean: blue, phase EH-I; orange, the coexistence of EH-I and EH-II phases; red, phase EH-II; green, decomposed ethylene in water. Dotted lines refer to spectra acquired on pure ethylene samples and are shown as a comparison. Pressure values are expressed in GPa. *Left:* Raman spectra in the 1280–1400 cm^{-1} frequency range, where the ν_3 vibration of ethylene ($-CH_2$ scissoring) can be found. The asterisks indicate the saturating Raman band from the diamond anvils. *Center:* Raman spectra in the ν_2 (C=C stretching) frequency range. *Right:* Raman spectra in the ν_1 and ν_5 frequency range, where the Raman bands for the symmetric and antisymmetric –C–H stretching modes of ethylene can be observed. The spectra have been normalized to the highest intensity and vertically shifted for the sake of clarity.

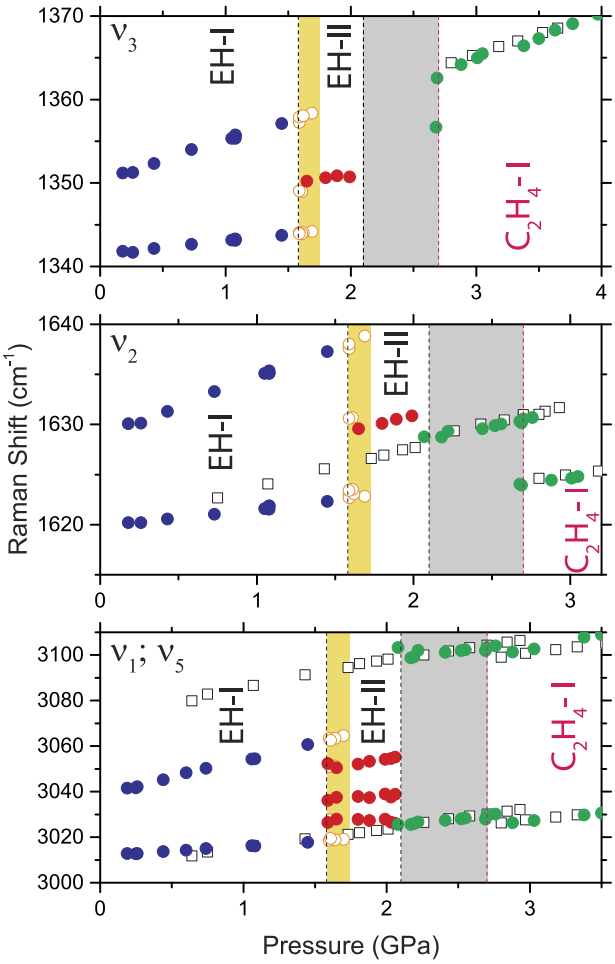

FIG. 3. Pressure evolution of the peak frequencies of ethylene Raman bands in the diverse clathrate hydrate phases with respect to pure ethylene. Solid blue circles: phase EH-I; open orange circles: coexistence of EH-I and EH-II phases; solid red circles: phase EH-II; solid green circles: decomposed ethylene in water. Black open squares refer to peak frequencies of pure ethylene and are shown as a comparison. The *Top*, *Middle*, and *Bottom* panels refer to ν_3, ν_2, and ν_1; ν_5 Raman modes of encaged ethylene, respectively. Vertical lines are intended as a guide for the eyes to locate the transition thresholds: black dotted lines refer (in order) to the EH-I to EH-II phase transition (1.60 GPa) and EH decomposition into ice and pure ethylene (2.10 GPa); pink dotted lines refer to the phase transition from phase II to phase I in pure ethylene. The yellow highlighted regions visually define the pressure range for the coexistence of EH-I and EH-II (1.60–1.75 GPa), while the gray highlighted regions visually define the pressure range where the clathrate structure disrupts into plastic C_2H_4 and water ice.

ν_3 and the C=C stretching ν_2 modes, and a better resolved structure, that can be reproduced using three components, in the region of the –C–H stretching ν_1 and ν_5 modes (see Fig. 2). This picture is quite consistent with the report by Shimizu *et al.*[24] Despite the evident similarities between the spectra in this phase and the spectra of the corresponding MH-II phase in the case of methane hydrate,[37] the lack of any dedicated structural study about EH-II allows only speculations about its actual structure.

At pressures exceeding 2.10 GPa, both the C=C and the –C–H stretching bands (see the green spectra in the central and right panels of Fig. 2; the $-CH_2$ scissoring band is covered by the saturating absorption of the diamond) become sharper and single-peaked, and we observe the second important transformation. This change is also highlighted by a darkening of the sample between 2.00 and 2.10 GPa [see pictures (c) and (d) in Fig. 1]. By the comparison of the Raman spectra acquired on the mixture (green curves in Fig. 2) with those acquired on a sample of pure ethylene (dotted curves), we assign this transformation to a decomposition of the ethylene clathrate hydrate into water ice and plastic C_2H_4-II. Starting from this pressure, the samples remained decomposed, and no spectral features suggesting the formation of any other kind of clathrate hydrate have been observed. In a pure ethylene sample, the ambient temperature phase transition between liquid and plastic ethylene lies at about 1.80 GPa; as soon as the EH-II decomposes, ethylene segregates in its plastic phase II in the presence of the excess water ice-VI (or ice-VII above 2.40 GPa). This structural evolution clearly emerges from the pressure evolution of the peak frequencies, which are reported in Fig. 3.

The observation of the decomposition of EH-II into its constituents calls into question the assignment of a third ethylene clathrate hydrate phase, EH-III, done by Shimizu and co-authors in the only other available work regarding the behavior of this system under moderate pressures (up to 3.16 GPa).[24] In that work, the authors claimed the existence of a *filled ice* EH-III structure, similar

to that of MH-III in methane hydrate, on the basis of a small frequency shift for the –C–H stretching band of the guest molecules. Nevertheless, this argument relied on a previous study by the same group,[38] where the decomposition of methane clathrate hydrate phase II into Ice-VI and solid-CH_4 was erroneously interpreted as the formation of the *filled ice* MH-III structure. As widely agreed in recent literature[37,39–42] and differently from what was reported by Shimizu *et al.*,[24] a much higher frequency shift is expected in the case of the formation of *filled ice* structures (about 10 cm^{-1}).

These results substantially change the picture of the phase diagram of ethylene clathrate hydrate, highlighting the existence of only two phases, EH-I (0.10–1.60 GPa) and EH-II (1.60–2.10 GPa), with a narrow pressure interval (1.60–1.75 GPa) where these two phases coexist, due to the sluggishness of the phase transition. Above 2.10 GPa, the sample decomposes into water ice and solid ethylene. These conclusions are further supported by the measured lattice phonon spectra we report in Fig. 4. Except for a few low-pressure points (P ≤ 0.50 GPa) reported by Sugahara *et al.*,[26] these Raman spectra are the first reported for the lattice phonons of ethylene hydrate. Figure 4 shows the lattice phonon region in the EH-I and EH-II phases and in their coexistence domain, together with the pressure evolution of their peak frequencies.

Despite the poor signal-to-noise ratio, possibly because of the presence of excess water and ethylene, the phonon spectra were successfully reproduced after background subtraction. Figure S1 included in the supplementary material reports an example of a spectral deconvolution for lattice phonons in phase EH-I. As it can be seen, EH-I phonon bands strictly remind the phonon spectrum of other sI-type structures such as methane clathrate hydrate,[37] thus confirming the initial assignment. As the sample enters the coexistence region between phases EH-I and EH-II, the phonon spectra become less readable, and we assist to an overall intensity reduction of the spectrum, as expected;[37] in general, only two broad bands are clearly visible. In addition, in the EH-II phase and differently from what was observed in the methane clathrate hydrate case, the spectrum seems to feature only two broad bands. These bands are compatible with the two most intense peaks observed in methane clathrate hydrate phase MH-II, and this can confidently lead us to assign this structure as similar to that of an sH-type clathrate.

Table S1 in the supplementary material collects the pressure shift coefficients of the lattice phonon and of the internal modes of encaged ethylene in the clathrate hydrate phases EH-I and EH-II as obtained from a linear fit of the frequency evolution with pressure (data reported in Fig. 3 and in the bottom panel of Fig. 4). Figure S2 shows, instead, our phonon data in continuity with those measured by Sugahara *et al.*[26] at lower pressures (below 0.50 GPa), highlighting how our most intense peak agrees with the behavior of the only lattice phonon reported in that work.

B. Water ices–ethylene crystals mixtures

The decomposed C_2H_4 and water solid ice mixture has been further compressed up to 15 GPa and heated in a range from room temperature up to 370 K. This allowed us to follow the pressure evolution of ethylene Raman bands, which we report in Figs. 5 and 6 for the very first time in this pressure range. Figure 5 reports the Raman spectra in the ν_2 (C=C stretching) and in the ν_1 and ν_5 (symmetric and antisymmetric –C–H stretching modes) frequency ranges,

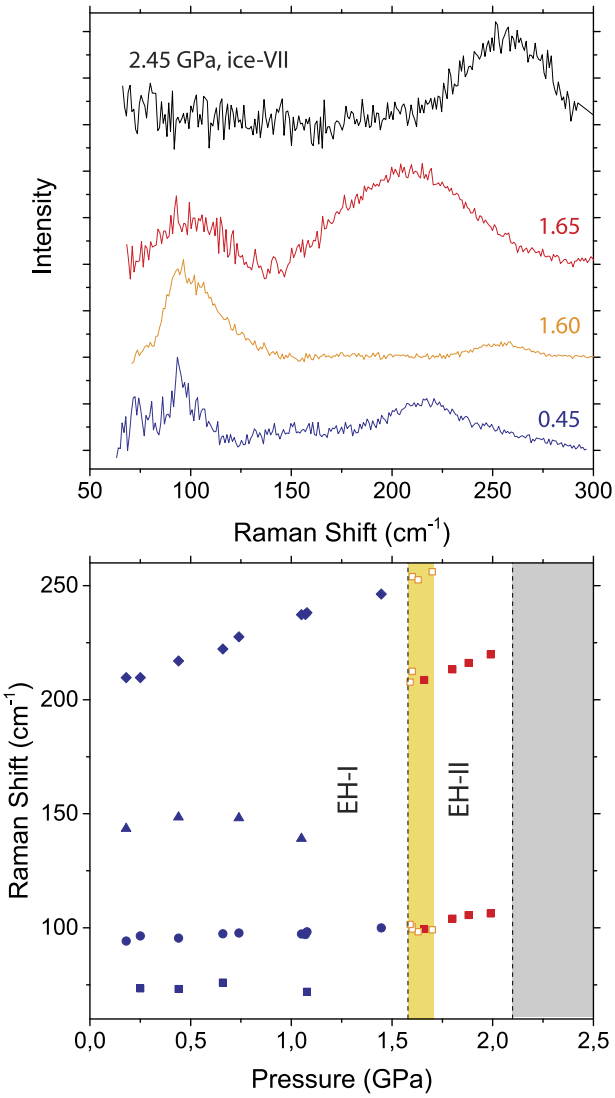

FIG. 4. *Top panel:* Lattice phonon spectra of ethylene clathrate hydrate in phase I (EH-I, blue curve), in the coexistence region of EH-I and EH-II (orange curve), and in phase II (EH-II, red curve). The black curve refers to a typical spectrum acquired after the ethylene hydrate decomposition (at 2.45 GPa), where the phonon bands of Ice-VII can be observed. Pressure values are expressed in GPa. The spectra have been normalized to the highest intensity and vertically translated for the sake of clarity. *Bottom panel:* Pressure evolution of the peak frequencies of the phonon bands of ethylene clathrate hydrate. Colors mean: solid blue, phase EH-I; open orange square, the coexistence of EH-I and EH-II phases; solid red, phase EH-II. Vertical, black dotted lines are intended as guides for the eyes to locate the various transition pressure; they refer in order to the EH-I to EH-II phase transition (1.60 GPa) and EH decomposition into ice and pure ethylene (2.10 GPa). The yellow highlighted area defines the region of coexistence for EH-I and EH-II (1.60–1.75 GPa), while the gray highlighted region visually defines the pressure range where the clathrate structure disrupts into plastic C_2H_4 and water ice.

while Fig. 6 reports the Raman spectra in the three relevant windows of the 0–1400 cm^{-1} region. For comparison, the spectra have been collected both on pure samples (black traces) and on ethylene in solid ice mixtures with water (green traces). The pressure

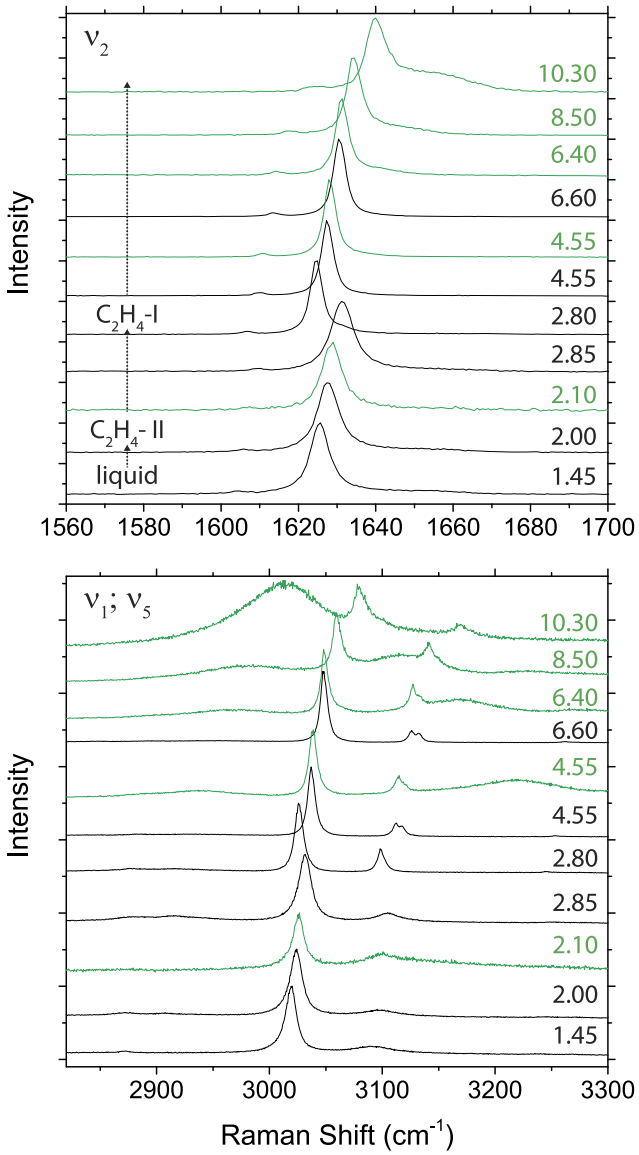

FIG. 5. Raman spectra of pure ethylene (black) compared to those acquired on the decomposed mixture of water and ethylene (green) at various pressures across liquid, plastic (C_2H_4-II), and fully ordered (C_2H_4-I) crystalline solid phases. *Top:* Raman spectra in the ν_2 (C=C stretching) frequency range. *Bottom:* Raman spectra in the ν_1 and ν_5 frequency range relative to the symmetric and antisymmetric –C–H stretching modes of ethylene. Pressure values are expressed in GPa. The spectra have been normalized to the highest intensity and vertically shifted for the sake of clarity.

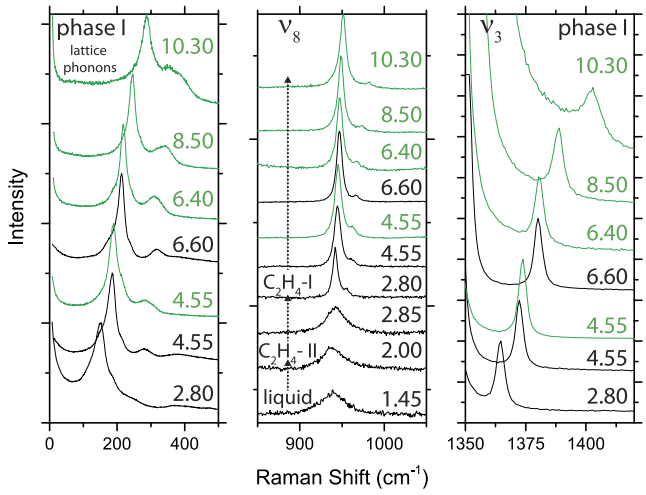

FIG. 6. Raman spectra of pure ethylene (black) compared to those acquired on the decomposed mixture of water and ethylene (green) at various pressures across liquid, plastic (C_2H_4-II), and fully ordered (C_2H_4-I) crystalline solid phases. *Left:* Raman spectra in the lattice phonon region. *Center:* Raman spectra in the ν_8 frequency range relative to the $-CH_2$ wagging mode. *Right:* Raman spectra in the ν_3 frequency range relative to the $-CH_2$ scissoring mode. Pressure values are expressed in GPa. The spectra have been normalized to the highest intensity and vertically shifted for the sake of clarity.

shifts of the Raman active internal and lattice phonon modes of pure ethylene are reported in Table S2 as obtained by a linear fit of the frequency evolution with pressure. These data are reported in Figs. S3 and S4 and are relative to the peak frequencies of the Raman bands of pure ethylene and of ethylene in water mixtures up to the highest investigated pressure. Notably, the aforementioned similarities between the spectra of the ethylene/water solid ice mixture and those of pure ethylene are confirmed by the pressure evolution of the frequencies of all the ethylene Raman peaks, which overlap those of pure ethylene up to the highest pressure where the monomer bands could be assigned in that sample, as already shown in Fig. 3 for the low pressure regime and in Fig. S3 for the whole range.

The liquid-to-plastic phase transition in C_2H_4 is somewhat elusive: it involves no evident frequency shifts, but it is highlighted in the –C–H stretching region by the intensification and sharpening of the ν_5 component (antisymmetric stretching). The ν_5 mode sharpens continuously up to the crystalline phase I, where, as previously reported in low temperature conditions,[18,19] it undergoes further splitting due to Davydov components at higher pressures (the same happens to the ν_1 band, becoming broader with pressure but remaining unresolved). A small frequency drop is systematically observed across the plastic C_2H_4-II to the crystalline C_2H_4-I phase transition. It is visible in the ν_2 mode related to C=C stretching (a frequency drop of about 6 cm^{-1}, from 1631 to 1625 cm^{-1}) and in the ν_1; ν_5 range, as mentioned earlier, but it is not observed in the $-CH_2$ wagging region (ν_8, Fig. 6). Here, the phase transition is indicated only by the sudden intensification and sharpening of the ν_8 Raman band, which in phase I features two distinct components at 946 and 967 cm^{-1}, respectively. This splitting, such as that aforementioned for the –C–H stretching bands, is expected in agreement with the crystal structure of monoclinic fully ordered C_2H_4-I, $P2_1/m$ with Z = 2 (two molecules per cell).[43,44] On the other hand, the splitting is far less visible in the C=C stretching band, where the single band observed in fluid and in plastic C_2H_4-II tends simply to become broader and slightly asymmetrical once the sample has transformed into phase I. Finally, the left and right panels in Fig. 6, respectively,

show the lattice phonon bands of solid ethylene and the $-CH_2$ scissoring band (ν_3). The $-CH_2$ scissoring band becomes visible only at high pressure; it is not observed in the liquid and plastic regimes. This does not mean that the $-CH_2$ scissoring is not active at lower pressures (it is indeed visible in the liquid phase spectra recorded at 113 K by Blumenfeld *et al.*[18]), but it is probably less intense and covered by the nearby, saturating absorption band of the diamond anvils. For what is concerned with the lattice phonon modes, basing on symmetry consideration, they are expected only in the fully ordered, crystalline monoclinic phase I (molecule point group D_{2h}, factor group C_i, and site group C_{2h}) but not in the cubic, orientationally disordered plastic phase II (where both factor and site group are O_h); in particular, in the case of C_2H_4-I, six Raman active librational modes are expected, four of which could be identified by the fit of the collected spectra (frequencies are reported in Fig. S4).

C. Polymerization in solid ice mixtures

Ethylene is reported to polymerize spontaneously at pressures exceeding 3.60 GPa at room temperature[20] or even lower at high temperatures[23] or under irradiation.[21,22] In these cases, infrared spectroscopy was employed as a probe to track the onset of the reaction and follow the reaction kinetics at constant pressure. IR is, indeed, very sensitive to the appearance of new absorption bands related to the polymer, while the bands from ethylene still remain visible after 300 h from the reaction onset.[20] Infrared spectroscopy was unsuitable for our samples due to their thickness, resulting in saturation of the main bands of both water and ethylene. On the other hand, Raman spectroscopy works as a point probe for the various regions of the sample; for instance, Raman allowed us to observe the first signs of a reaction in different areas of the sample already around 2.85 GPa, on the threshold of the plastic-to-ordered phase transition, and at a significantly lower pressure than expected, although a possible contribution to the reaction from the laser light cannot be excluded. Taking into account these differences between the probes used to follow the process, we were able to track the high pressure/high temperature behavior of the solid ice mixture of water and ethylene and to compare it with the pure system. The results are summarized in Fig. 7. First, we delimited the field of existence of the solid ice mixtures, trying to constrain the p, T region in which the ethylene monomer remains stable and does not completely convert into the polymer. Based on the results of room temperature compressions and on a high temperature isothermal compression (open green circles in Fig. 7), the ethylene bands persist up to 10.50 GPa. The fact that this pressure value was found both at room temperature and at a high temperature clearly indicates that this threshold is temperature-independent. Figure 7 also reports the reaction threshold observed along a series of isobaric heatings performed on the solid ice mixture (solid green circles) and on pure ethylene samples (solid gray diamonds).

While the threshold for the polymerization reaction in pure ethylene samples heated at 4.20 and 8.00 GPa (the gray diamonds in Fig. 7) roughly follows the phase boundary between ethylene phases I and II as analytically reproduced from the experimental points,[20,23,45–47] thus suggesting a topochemical reaction triggered by lattice phonons in phase I,[20] the solid–solid

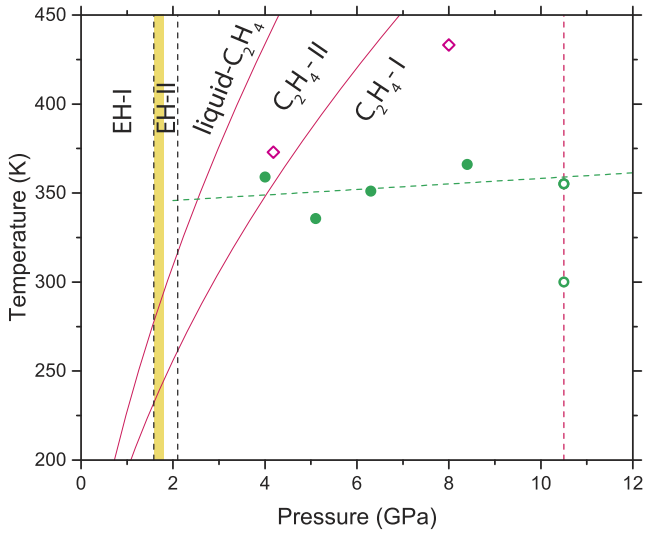

FIG. 7. Phase diagram of pure ethylene, as indicated by the solid pink lines (curve analytically reproduced from the experimental data related to the transition from liquid to plastic phase II and from plastic phase II to fully ordered crystalline phase I).[20,23,45–47] The dotted black lines refer to the ethylene clathrate hydrate phase diagram, highlighting the EH-I to EH-II phase transition and the hydrate decomposition threshold. The yellow highlighted regions visually define the pressure range for the coexistence of EH-I and EH-II (1.60–1.75 GPa). Superimposed on the phase diagrams, the experimental p, T threshold measured in this work in relation to ethylene polymerization in pure solid phase (magenta diamonds) and in ethylene/water mixtures (green circles). Open green circles indicate the pressure threshold obtained in two distinct compression experiments at room temperature and at high temperature (355.15 K). The dotted green line is a guide for the eyes, indicating the behavior of the threshold line in ethylene/water mixtures, while the vertically dotted pink line highlights the polymerization threshold in pressure as obtained in this experiment.

mixture behaves quite differently. The high temperature/high pressure polymerization threshold follows the green dotted line reported in Fig. 7, lying well below the I–II phase transition in pure ethylene. Its slope suggests that the threshold is independent of pressure in the investigated p, T range, thus representing a kinetic boundary. The green line is just a guide to the eye following the threshold temperatures measured during the heating at 4.00, 5.10, 6.30, and 8.40 GPa (green circles in Fig. 7) and that of the isothermal compression at 355.1 K (open green circles). Figure S5 reports two sequences of Raman spectra acquired during the heating at two different pressures; from these data, we derived the threshold temperatures reported in Fig. 7 as the temperatures where the bands related to –C–H stretching of polyethylene drastically intensified.

The peculiar threshold line measured in the solid ice mixture with respect to what is expected in the case of pure molecular crystals (see, for instance, the case of pure ethylene[23]) can be ascribed to the arrangement of water and ethylene in the ice mixture, probably consisting in variously dimensioned C_2H_4 crystalline clusters surrounded by water ice regions. In bulk processes for pure molecular crystals, the reaction trigger is identified in the collective processes related to the lattice phonon motions; pressure keeps molecules closer to each other and forces them to interact,

while temperature widens the molecular motions.[48] In small clusters, the reactivity can be heavily modified by surface effects, local stress, or anisotropy. This idea is also supported considering that, on decompression, the reaction significantly accelerates in all the samples; this observation was not made in pure ethylene, and it can be ascribed to deformations induced by the stress to the reaction cavity.[49]

The finely dispersed ethylene crystallites are likely characterized by pronounced local disorder, although their Raman spectra tell us that they preserve long range translational order. This picture explains the production of highly defective polymers resulting from the analysis of the recovered polyethylenes. Figure 8 reports the infrared spectra acquired on the representative recovered polyethylenes from ice mixtures, while Fig. 9 reports the XRD patterns and the Raman spectra of the same polymers. As can be easily seen, the products encompass the intermediate characteristics of various amorphous and low density polyethylenes. A summary of the vibrational bands measured on polyethylene (both IR and Raman active) can be found in Table S3 in the supplementary material.

In Fig. 8, a sequence of infrared spectra recorded in the four significant spectral regions is reported. In these four regions, all the products obtained from the ethylene/water mixture present spectroscopic features that can be related to amorphous, low-density polymers. The $-CH_2$ rocking doublet ranges from a quite well resolved (blue and red traces) to a very poorly resolved shape (green trace). On the other hand, all the spectra of the recovered polyethylenes obtained from the ethylene/water mixtures present a sharp band at 1378 cm^{-1}, characteristic of symmetric bending modes of $-CH_3$ groups. This clearly indicates that in our products a large amount of chain terminations are found, and so the polymeric chains have to

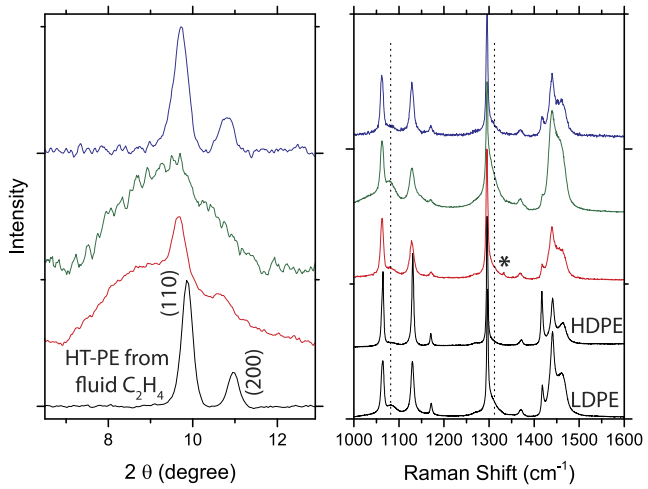

FIG. 9. X-ray diffraction patterns and Raman spectra acquired on the recovered polyethylene from ethylene in solid ice mixtures with water. *Left panel:* limit cases of XRD patterns of polyethylene as obtained from the mixture (green, red, and blue curves) compared to the XRD pattern of polyethylene obtained from the high temperature polymerization of fluid ethylene[23] (black curve). All the patterns have been measured with λ = 0.710 73 Å and are vertically shifted for the sake of clarity. *Right Panel:* limit cases of Raman spectra obtained from the polymerization of ethylene in the mixture with water (green, red, and blue curves) compared to the Raman spectra measured on commercial low-density polyethylene (LDPE) and high-density polyethylene (HDPE) from Sigma-Aldrich.[20] The dotted lines indicate the broad Raman bands at 1078 and 1310 cm^{-1} observed in low-density polyethylene, while the asterisk locates the unexpected, extra Raman band at 1332 cm^{-1} that is observed in some of the recovered samples. The spectra are normalized to the most intense peak and vertically shifted for the sake of clarity.

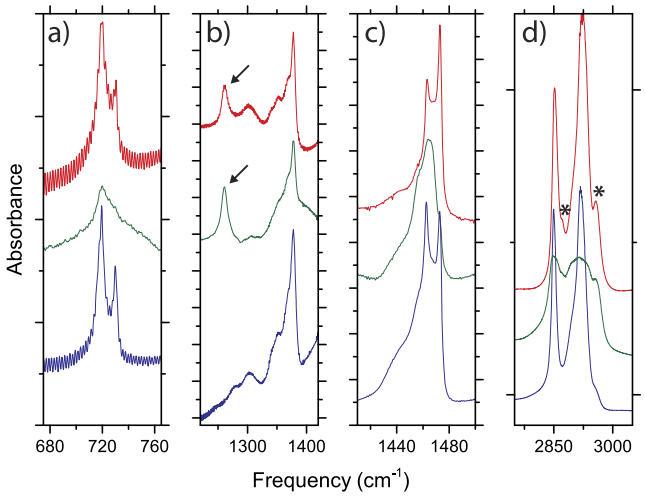

FIG. 8. IR spectra on the recovered samples of polyethylene as obtained from ethylene in solid ice mixtures with water in four relevant spectral regions, from left to right: (a) in the $-CH_2$ rocking mode region; (b) in the $-CH_2$ wagging and twisting region; (c) in the $-CH_2$ bending region; and (d) in the $-CH_2$ stretching region. The blue, green, and red curves refer to limit cases among the obtained products. Arrows in panel (b) and asterisks in panel (d) refer to peculiar spectral features of the recovered products. Spectra are vertically shifted for the sake of clarity.

be considered relatively short and branched, consistently with the small extensions of the hydrocarbon crystalline clusters. Furthermore, in several of our recovered spectra, we did observe a sharp, well defined band at 1260 cm^{-1} [highlighted by arrows in panel (b) of Fig. 8, green and red traces]. A similar band can be expected in the presence of *cis*-dialkyl ethylenes (RH–C=C–RH) groups, and it is due to in-plane –CH group deformations.[50] This attests to an incomplete polymerization in some of our products and reveals the formation of isolated chains that get progressively connected upon releasing pressure while recovering the product at ambient conditions. In the 1420–1500 cm^{-1} spectral range, we have differently resolved doublets and a broad band at 1440 cm^{-1}. Moreover, in all the spectra, we observe a broad shoulder centered approximately at 1455 cm^{-1}, related to the antisymmetric bending mode of $-CH_3$ groups,[51] confirmation of the presence of chain terminations. Looking at the panel (d) in Fig. 8, we see that, beyond the expected bands of the $-CH_2$ stretching modes, we have the stretching bands due to the –C–H in the terminal $-CH_3$ groups (symmetric and antisymmetric ones, at 2870 and 2960 cm^{-1}, highlighted by asterisks on the red trace). On the other hand, in some other products, the peaks in this region are very stressed, and the well defined –C–H stretching components collapse into a broader band (see green trace).

The picture obtained through the analysis of infrared data was confirmed by the Raman spectra of the recovered polyethylenes

(see the right panel in Fig. 9) as compared with those of commercial high-density (HD) and low-density (LD) polyethylenes from Sigma-Aldrich.[20] The spectra feature all the expected active bands for polyethylene,[52–56] whose assignment is reported in full detail in Table S3. Moreover, as expected for the low-density polymer, we always observed large bands at 1078 and 1310 cm^{-1}, related to C–C bending and $–CH_2$ twisting modes in the amorphous polymer, respectively. In all of our products' spectra, the lower frequency component of the $–CH_2$ bending structure at 1418 cm^{-1} has a very low intensity and it is poorly resolved (except maybe for the blue trace). The intensity of this band and its definition with respect to the higher frequency doublet are reported to increase with the density and the degree of crystallinity of the polymer,[52,57] which confirms the disorder of our products as found in the IR analysis. Finally, in the green trace of the right panel in Fig. 9, a small band at 1332 cm^{-1}, highlighted by an asterisk, is also visible. This band could be related to $–CH_3$ deformations,[50,52] thus further attesting to the presence of short chains.

The x-ray diffraction patterns acquired on the recovered polyethylenes are reported in the left panel of Fig. 9 in comparison with the very high quality polyethylene obtained from the high temperature polymerization of fluid ethylene.[23] As it can be seen, despite some better cases (the blue curve), more often we obtained an amorphous polymer with only some remnants of the two main orthorhombic *Pnma* polyethylene reflections, (110) and (200), as in the red curve, or just a broad, weak peak as in the green trace, characteristics of a completely amorphous material in good agreement with existing literature.[58–60]

The presence of differently defected polyethylenes as recovered products could be explained by the formation of ethylene crystallites of quite different dimensions in the solid ice mixture following the decomposition of the pristine ethylene clathrate hydrate. In this framework, depending on the actual dimensions of these clusters, we obtained products ranging from polymers of quite good quality to highly defected, largely branched and amorphous materials, with lots of terminations, shorter lengths and, in some cases, not completely transformed, resulting in residual unsaturated C=C groups along the chains. It is quite unlikely that these differences could be related to some kind of inclusion of the hydrocarbon within the ice network; indeed, ice-VII is a very dense polymorphic type of water ice, and it is not known to host guest molecules as cumbersome as ethylene, differently from what happens for more penetrable polymorphs (i.e., at the phase transition between amorphous and crystalline water ice[61]). It can be concluded that in our samples we often had largely inhomogeneous distributions of water and ethylene domains in the form of small clusters, further stressed by compression, and that this condition is at the origin of the obtained low density polyethylenes. On the basis of the available data, it is difficult to figure out whether water plays an active role in the whole process other than contributing to establish the peculiar reaction cavity in which the polymerization occurs; in this regard, the lowering of the temperature threshold for the polymerization with respect to bulk polyethylene can be explained as a kinetic effect related to the local stress, while the persistence of ethylene at pressures higher than those reported in previous literature can be attributed both to the compression anisotropy or to the scarce sensitivity of the probe technique (Raman) toward the reaction onset.

IV. CONCLUSIONS

In this experimental work, we studied the behavior of ethylene–water mixtures in a pressure range from 0 to 15 GPa and with temperature varying between 300 and 370 K. First, we observed the pressure evolution of ethylene clathrate hydrate (EH) up to its decomposition threshold at about 2.10 GPa. After that, the evolution of the decomposed ethylene–water solid–solid ice mixture was studied. We found over a number of experiments that the only two stable polymorphs for ethylene hydrate are the caged structures EH-I (sI-type) and EH-II (presumably s-H type), with no evidence of the *filled ice*-like phase EH-III previously reported.[24] Instead of this third phase, we observed the decomposition of the ethylene clathrate hydrate into a solid ice mixture of ethylene and water, finely dispersed and mixed into variously dimensioned ethylene crystallites. Raman signatures of ethylene were observed up to 10.5 GPa, where the bands from the monomer disappeared and the complete transformation to the polymer was achieved. This can be explained by the compression anisotropy, increasing at high pressure, but it could also be due to the scarce sensitivity of Raman toward the detection of the reaction onset.

For what concerns the high-temperature behavior of the ethylene–water mixture, we measured a threshold line for the polymerization reaction of ethylene that is not dependent on pressure and significantly lower than the transition line between fully ordered C_2H_4-I and plastic C_2H_4-II crystalline phases, where the polymerization seems to be complete in the case of pure ethylene samples. This threshold in solid ice mixtures appears to be a kinetic boundary, purely related to the local stress exerted by the arrangement of ethylene and water in the shape of variously dimensional crystalline clusters. Crystal dimensions play the greatest role also in determining the quality of the recovered polyethylenes; the crystalline quality of polymers appears indeed to be mainly correlated with cluster dimensions instead of reaction pressure and temperature conditions. In any case, we obtained differently defected polyethylenes featuring very low density, short chains, lots of terminations, and branching.

Complex ice mixtures involving hydrocarbons are widespread in our universe, and their properties may differ significantly from those of the pure constituents; the results obtained in these experiments are therefore pivotal to a deeper understanding of ethylene–water system behavior at high pressure and temperature in several astrochemical contexts, both as clathrate hydrates and as solid ice mixtures. This study, which encompasses a variety of topics ranging from the structural evolution of the hydrate phases to the study of ice mixtures in terms of their structure and their pressure-/temperature-induced reactivity, is significant also in terms of fundamental science, providing new insights and perspectives to modelize the behavior of real, widely distributed complex systems. Finally, the formation of a soft, low density polyethylene from the ethylene/water mixtures, characterized by a waxy appearance and, possibly, a high porosity, is obviously interesting as polyethylene is a widely-studied benchmark polymer for technology applications. More studies would be necessary to better characterize the behavior of ethylene/water mixtures at lower temperatures and to refine the structural features of ethylene clathrate hydrate phase EH-II, which is currently not assigned.

SUPPLEMENTARY MATERIAL

See the supplementary material for additional data about ethylene clathrate hydrate, as well as pure ethylene and ethylene/water solid ice mixtures.

ACKNOWLEDGMENTS

This study was supported by the Deep Carbon Observatory (DCO) initiative under the project Physics and Chemistry of Carbon at Extreme Conditions, by the Italian Ministero dell'Istruzione, dell'Università e della Ricerca (MIUR), and by the Fondazione Cassa di Risparmio di Firenze under the project HP-PHOTOCHEM.

AUTHOR DECLARATIONS

Conflict of Interest

The authors have no conflicts to disclose.

Author Contributions

S. Berni: Data curation (equal); Investigation (equal); Writing – review & editing (equal). **D. Scelta**: Conceptualization (equal); Data curation (equal); Investigation (equal); Writing – original draft (lead); Writing – review & editing (equal). **S. Fanetti**: Conceptualization (equal); Investigation (equal); Writing – review & editing (equal). **R. Bini**: Conceptualization (equal); Resources (lead); Supervision (lead); Writing – review & editing (equal).

DATA AVAILABILITY

The data that support the findings of this study are available from the corresponding author upon reasonable request.

REFERENCES

[1]E. F. van Dishoeck, E. Herbst, and D. A. Neufeld, "Interstellar water chemistry: From laboratory to observations," Chem. Rev. **113**, 9043–9085 (2013).
[2]P. Ehrenfreund and H. Fraser, "Ice chemistry in space," in *Solid State Astrochemistry*, edited by V. Pirronello, J. Krelowski, and G. Manicò (Springer, Netherlands, Dordrecht, 2003), pp. 317–356.
[3]H. Hussmann, C. Sotin, and J. I. Lunine, "10.18 - interiors and evolution of icy satellites," in *Treatise on Geophysics*, 2nd ed., edited by G. Schubert (Elsevier, Oxford, 2015), pp. 605–635.
[4]M. E. Brown, "The compositions of Kuiper belt objects," Annu. Rev. Earth Planet. Sci. **40**, 467–494 (2012).
[5]H. Y. McSween, Jr and G. R. Huss, *Cosmochemistry* (Cambridge University Press, 2010).
[6]F. Nimmo and R. T. Pappalardo, "Ocean worlds in the outer solar system," J. Geophys. Res. Planets **121**, 1378–1399, https://doi.org/10.1002/2016je005081 (2016).
[7]A. M. Shaw, *Astrochemistry: From Astronomy to Astrobiology*, 1st ed. (Wiley, 2006).
[8]M. H. Moore and R. L. Hudson, "Infrared study of ion-irradiated water-ice mixtures with hydrocarbons relevant to comets," Icarus **135**, 518–527 (1998).
[9]M. Ceppatelli and R. Bini, "Light-induced catalyst and solvent-free high pressure synthesis of high density polyethylene at ambient temperature," Macromol. Rapid Commun. **35**, 787–793 (2014).
[10]E. C. Czaplinski, W. A. Gilbertson, K. K. Farnsworth, and V. F. Chevrier, "Experimental study of ethylene evaporites under Titan conditions," ACS Earth Space Chem. **3**, 2353–2362 (2019).
[11]S. Singh, J.-P. Combe, D. Cordier, A. Wagner, V. F. Chevrier, and Z. McMahon, "Experimental determination of acetylene and ethylene solubility in liquid methane and ethane: Implications to Titan's surface," Geochim. Cosmochim. Acta **208**, 86–101 (2017).
[12]H. G. Roe, I. de Pater, and C. P. McKay, "Seasonal variation of Titan's stratospheric ethylene C_2H_4 observed," Icarus **169**, 440–461 (2004).
[13]B. E. Hesman, G. L. Bjoraker, P. V. Sada, R. K. Achterberg, D. E. Jennings, P. N. Romani, A. W. Lunsford, L. N. Fletcher, R. J. Boyle, A. A. Simon-Miller, C. A. Nixon, and P. G. J. Irwin, "Elusive ethylene detected in Saturn's northern storm region," Astrophys. J. **760**, 24 (2012).
[14]P. N. Romani, D. E. Jennings, G. L. Bjoraker, P. V. Sada, G. H. McCabe, and R. J. Boyle, "Temporally varying ethylene emission on Jupiter," Icarus **198**, 420–434 (2008).
[15]M. E. Brown, E. L. Schaller, and G. A. Blake, "Irradiation products on dwarf planet Makemake," Astron. J. **149**, 105 (2015).
[16]G. R. Gladstone, S. A. Stern, K. Ennico, C. B. Olkin, H. A. Weaver, L. A. Young, M. E. Summers, D. F. Strobel, D. P. Hinson, J. A. Kammer, A. H. Parker, A. J. Steffl, I. R. Linscott, J. W. Parker, A. F. Cheng, D. C. Slater, M. H. Versteeg, T. K. Greathouse, K. D. Retherford, H. Throop, N. J. Cunningham, W. W. Woods, K. N. Singer, C. C. C. Tsang, R. Schindhelm, C. M. Lisse, M. L. Wong, Y. L. Yung, X. Zhu, W. Curdt, P. Lavvas, E. F. Young, G. L. Tyler, F. Bagenal, W. M. Grundy, W. B. McKinnon, J. M. Moore, J. R. Spencer, T. Andert, J. Andrews, M. Banks, B. Bauer, J. Bauman, O. S. Barnouin, P. Bedini, K. Beisser, R. A. Beyer, S. Bhaskaran, R. P. Binzel, E. Birath, M. Bird, D. J. Bogan, A. Bowman, V. J. Bray, M. Brozovic, C. Bryan, M. R. Buckley, M. W. Buie, B. J. Buratti, S. S. Bushman, A. Calloway, B. Carcich, S. Conard, C. A. Conrad, J. C. Cook, D. P. Cruikshank, O. S. Custodio, C. M. D. Ore, C. Deboy, Z. J. B. Dischner, P. Dumont, A. M. Earle, H. A. Elliott, J. Ercol, C. M. Ernst, T. Finley, S. H. Flanigan, G. Fountain, M. J. Freeze, J. L. Green, Y. Guo, M. Hahn, D. P. Hamilton, S. A. Hamilton, J. Hanley, A. Harch, H. M. Hart, C. B. Hersman, A. Hill, M. E. Hill, M. E. Holdridge, M. Horanyi, A. D. Howard, C. J. A. Howett, C. Jackman, R. A. Jacobson, D. E. Jennings, H. K. Kang, D. E. Kaufmann, P. Kollmann, S. M. Krimigis, D. Kusnierkiewicz, T. R. Lauer, J. E. Lee, K. L. Lindstrom, A. W. Lunsford, V. A. Mallder, N. Martin, D. J. McComas, R. L. McNutt, D. Mehoke, T. Mehoke, E. D. Melin, M. Mutchler, D. Nelson, F. Nimmo, J. I. Nunez, A. Ocampo, W. M. Owen, M. Paetzold, B. Page, F. Pelletier, J. Peterson, N. Pinkine, M. Piquette, S. B. Porter, S. Protopapa, J. Redfern, H. J. Reitsema, D. C. Reuter, J. H. Roberts, S. J. Robbins, G. Rogers, D. Rose, K. Runyon, M. G. Ryschkewitsch, P. Schenk, B. Sepan, M. R. Showalter, M. Soluri, D. Stanbridge, T. Stryk, J. R. Szalay, M. Tapley, A. Taylor, H. Taylor, O. M. Umurhan, A. J. Verbiscer, M. H. Versteeg, M. Vincent, R. Webbert, S. Weidner, G. E. Weigle, O. L. White, K. Whittenburg, B. G. Williams, K. Williams, S. Williams, A. M. Zangari, and E. Zirnstein, "The atmosphere of pluto as observed by new horizons," Science **351**, aad8866 (2016).
[17]C. A. Griffith, B. Bézard, T. K. Greathouse, D. M. Kelly, J. H. Lacy, and K. S. Noll, "Thermal infrared imaging spectroscopy of Shoemaker–Levy 9 impact sites: Spatial and vertical distributions of NH_3, C_2H_4, and 10-μm dust emission," Icarus **128**, 275–293 (1997).
[18]S. M. Blumenfeld, S. P. Reddy, and H. L. Welsh, "Vibrational Raman spectra of liquid and solid ethylene," Can. J. Phys. **48**, 513–520 (1970).
[19]G. R. Elliott and G. E. Leroi, "Raman study of crystalline ethylenes and the structure determination through model calculations of the lattice spectra," J. Chem. Phys. **59**, 1217–1227 (1973).
[20]D. Chelazzi, M. Ceppatelli, M. Santoro, R. Bini, and V. Schettino, "Pressure-induced polymerization in solid ethylene," J. Phys. Chem. B **109**, 21658–21663 (2005).
[21]D. Chelazzi, M. Ceppatelli, M. Santoro, R. Bini, and V. Schettino, "High-pressure synthesis of crystalline polyethylene using optical catalysis," Nat. Mater. **3**, 470–475 (2004).
[22]S. Romi, S. Fanetti, and R. Bini, "Accessing the activation mechanisms of ethylene photo-polymerization under pressure by transient infrared absorption spectroscopy," J. Phys. Chem. B **124**, 8149–8157 (2020).
[23]D. Scelta, M. Ceppatelli, and R. Bini, "Pressure induced polymerization of fluid ethylene," J. Chem. Phys. **145**, 164504 (2016).

[24]H. Shimizu, N. Tada, R. Ikawa, T. Kume, and S. Sasaki, "Optical microscopy and in situ Raman scattering of single crystalline ethylene hydrate and binary methane-ethylene hydrate at high pressures," J. Phys. Chem. B **109**, 22285–22289 (2005).
[25]E. Dartois, "Infrared spectroscopy of clathrate hydrates for planetary science: The ethylene case," Mon. Not. R. Astron. Soc. **504**, 4369–4376 (2021).
[26]T. Sugahara, K. Morita, and K. Ohgaki, "Stability boundaries and small hydrate-cage occupancy of ethylene hydrate system," Chem. Eng. Sci. **55**, 6015–6020 (2000).
[27]S. Takeya and A. Hachikubo, "Distortion of the host water cages of structure I gas hydrates: Structural analysis of C_2H_4 hydrate by powder X-ray diffraction," J. Phys. Chem. C **125**, 28150–28156 (2021).
[28]S. Fanetti, D. Scelta, and R. Bini, "Growth dynamics of crystalline Ar hydrate," J. Phys. Chem. C **124**, 10159–10166 (2020).
[29]H. K. Mao, P. M. Bell, J. W. Shaner, and D. J. Steinberg, "Specific volume measurements of Cu, Mo, Pd, and Ag and calibration of the ruby R_1 fluorescence pressure gauge from 0.06 to 1 Mbar," J. Appl. Phys. **49**, 3276–3283 (1978).
[30]K. Syassen, "Ruby under pressure," High Pressure Res. **28**, 75–126 (2008).
[31]D. Scelta, M. Ceppatelli, R. Ballerini, A. Hajeb, M. Peruzzini, and R. Bini, "Spray-loading: A cryogenic deposition method for diamond anvil cell," Rev. Sci. Instrum. **89**, 053903 (2018).
[32]M. Ceppatelli, F. A. Gorelli, J. Haines, M. Santoro, and R. Bini, "Probing high-pressure reactions in heterogeneous materials by Raman spectroscopy," Z. Kristallogr. - Cryst. Mater. **229**, 83–91 (2014).
[33]M. Santoro, A. Hajeb, and F. A. Gorelli, "Resistively heated, high pressure, membrane and screw driven diamond anvil cell," High Pressure Res. **40**, 379–391 (2020).
[34]M. Wojdyr, "*Fityk*: A general-purpose peak fitting program," J. Appl. Cryst. **43**, 1126–1128 (2010).
[35]R. Bini, R. Ballerini, G. Pratesi, and H. J. Jodl, "Experimental setup for Fourier transform infrared spectroscopy studies in condensed matter at high pressure and low temperatures," Rev. Sci. Instrum. **68**, 3154–3160 (1997).
[36]C. Prescher and V. B. Prakapenka, "Dioptas: A program for reduction of two-dimensional X-ray diffraction data and data exploration," High Pressure Res. **35**, 223–230 (2015).
[37]D. Scelta, S. Fanetti, S. Berni, M. Ceppatelli, and R. Bini, "Addressing open issues about the structural evolution of methane clathrate hydrate," J. Phys. Chem. C **126**, 19487–19495 (2022).
[38]H. Shimizu, T. Kumazaki, T. Kume, and S. Sasaki, "In situ observations of high-pressure phase transformations in a synthetic methane hydrate," J. Phys. Chem. B **106**, 30–33 (2002).
[39]H. Hirai, Y. Uchihara, H. Fujihisa, M. Sakashita, E. Katoh, K. Aoki, K. Nagashima, Y. Yamamoto, and T. Yagi, "High-pressure structures of methane hydrate observed up to 8 GPa at room temperature," J. Chem. Phys. **115**, 7066–7070 (2001).
[40]T. Ohtani, Y. Ohno, S. Sasaki, T. Kume, and H. Shimizu, "High-pressure Raman study of methane hydrate 'filled ice,'" J. Phys. Conf. Ser. **215**, 012058 (2010).
[41]J.-Y. Chen and C.-S. Yoo, "Formation and phase transitions of methane hydrates under dynamic loadings: Compression rate dependent kinetics," J. Chem. Phys. **136**, 114513 (2012).
[42]L. Bezacier, E. Le Menn, O. Grasset, O. Bollengier, A. Oancea, M. Mezouar, and G. Tobie, "Experimental investigation of methane hydrates dissociation up to 5 GPa: Implications for Titan's interior," Phys. Earth Planet. Inter. **229**, 144–152 (2014).
[43]W. Press and J. Eckert, "Structure of solid ethylene-d_4," J. Chem. Phys. **65**, 4362–4364 (1976).
[44]G. J. H. Nes and A. Vos, "Single-crystal structures and electron density distributions of ethane, ethylene and acetylene. III. Single-crystal X-ray structure determination of ethylene at 85 K," Acta Crystallogr., Sect. B: Struct. Sci., Cryst. Eng. Mater. **35**, 2593–2601 (1979).
[45]H. Wieldraaijer, J. A. Schouten, and N. J. Trappeniers, "Investigation of the phase diagrams of ethane, ethylene, and methane at high pressures," High Temp. High Pressure **15**, 87–92 (1983).
[46]N. J. Trappeniers and F. A. S. Ligthart, "Proton spin relaxation in ethylene. 'A new high pressure phase,'" Chem. Phys. Lett. **19**, 465–470 (1973).
[47]L. van der Putten, J. A. Schouten, and N. J. Trappeniers, "A differential scanning calorimetry study of ethylene and propane up to 10 kbar: The phase diagram of ethylene up to 23 kbar," High Temp. High Pressure **18**, 255–264 (1986).
[48]L. Ciabini, M. Santoro, F. A. Gorelli, R. Bini, V. Schettino, and S. Raugei, "Triggering dynamics of the high-pressure benzene amorphization," Nat. Mater. **6**, 39–43 (2006).
[49]R. Bini and V. Schettino, *Materials Under Extreme Conditions* (Imperial College Press, 2014).
[50]D. Lin-Vien, N. B. Colthup, W. G. Fateley, and J. G. Grasselli, *The Handbook of Infrared and Raman Characteristic Frequencies of Organic Molecules* (Academic Press, 1991).
[51]S. Krimm, "Infrared spectra of high polymers," *Fortschritte Der Hochpolymeren-Forschung* (Springer, Berlin, Heidelberg, 1960), pp. 51–172.
[52]K. Sano, M. Shimoyama, M. Ohgane, H. Higashiyama, M. Watari, M. Tomo, T. Ninomiya, and Y. Ozaki, "Fourier transform Raman spectra of linear low-density polyethylene and prediction of their density by multivariate data analysis," Appl. Spectrosc. **53**, 551–556 (1999).
[53]M. J. Gall, P. J. Hendra, O. J. Peacock, M. E. A. Cudby, and H. A. Willis, "The laser-Raman spectrum of polyethylene: The assignment of the spectrum to fundamental modes of vibration," Spectrochim. Acta, Part A **28**, 1485–1496 (1972).
[54]J. Maxfield, R. S. Stein, and M. C. Chen, "Polarized Raman studies of crystalline and amorphous orientation in polyethylene," J. Polym. Sci., Polym. Phys. Ed. **16**, 37–48 (1978).
[55]R. P. Wool, R. S. Bretzlaff, B. Y. Li, C. H. Wang, and R. H. Boyd, "Infrared and Raman spectroscopy of stressed polyethylene," J. Polym. Sci., Part B: Polym. Phys. **24**, 1039–1066 (1986).
[56]K. P. J. Williams and N. J. Everall, "Use of micro Raman spectroscopy for the quantitative determination of polyethylene density using partial least-squares calibration," J. Raman Spectrosc. **26**, 427–433 (1995).
[57]G. R. Strobl and W. Hagedorn, "Raman spectroscopic method for determining the crystallinity of polyethylene," J. Polym. Sci., Polym. Phys. Ed. **16**, 1181–1193 (1978).
[58]M. Kresteva, E. Nedkov, E. Sinigerska, and V. Krestev, "Phase composition of nascent and thermal-treated superhigh-molecular-weight polyethylene investigated by wide-angie X-ray diffraction at stepwise increased temperature," J. Macromol. Sci. Phys. **21**, 383–396 (1982).
[59]J. E. Preedy and E. J. Wheeler, "A study of structural order in various polyethylenes at elevated temperatures," Makromol. Chem. **178**, 2461–2470 (1977).
[60]D. C. Bassett, S. Block, and G. J. Piermarini, "A high-pressure phase of polyethylene and chain-extended growth," J. Appl. Phys. **45**, 4146–4150 (1974).
[61]A. Lignell and M. S. Gudipati, "Mixing of the immiscible: Hydrocarbons in water-ice near the ice crystallization temperature," J. Phys. Chem. A **119**, 2607–2613 (2015).